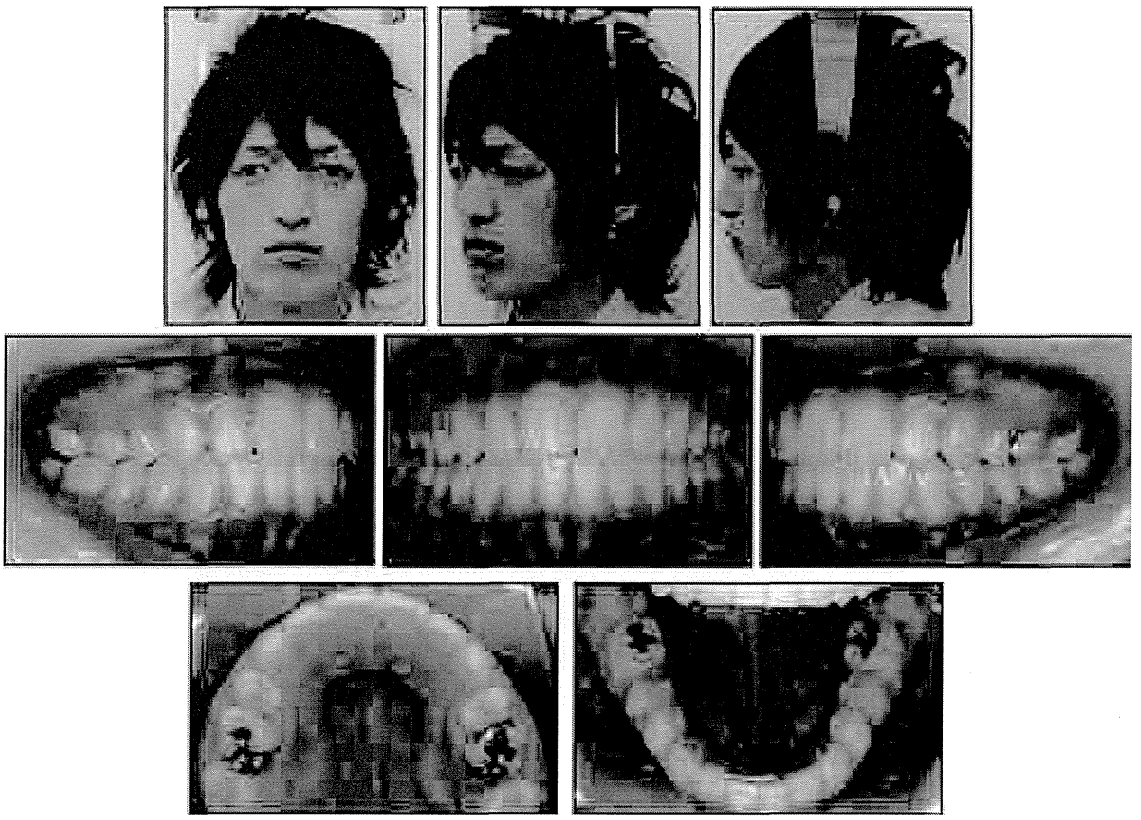

Fig 10. Posttreatment photographs (9 years after the distraction osteogenesis).

cephalometric tracings before and after distraction, the posterior nasal spine was moved significantly downward, even though we carefully controlled the direction of maxillofacial advancement using 2 protraction devices placed at orbitale and the maxilla. Generally, it is important to maintain the vertical height of the midface during LeFort III distraction osteotomy as soon as possible, because downward movement of the maxillofacial complex accelerates clockwise rotation of the mandible and causes reduced overbite. In our patient, the mandible was slightly rotated downward; however, it contributed to improving his deep overbite.

At 3 years after initiating retention, the maxillary incisors were lingually inclined, and the excessive overjet was corrected. Shetye et al[21] suggested that the retropositioning of the maxillary incisal edges might be explained by the changes in lip and tongue posture and the increased lip pressure on the maxillary incisors after the midface advancement. The mandibular plane angle was slightly decreased during the 3 years of retention.

In the cephalometric evaluation at 9 years after distraction, no relapse of the maxillofacial advancement was found, and both anteroposterior and vertical growth of the maxillofacial complex were observed. It might not be adequate to recognize this as real growth, because we used a protraction headgear for 6 years after distraction for both retention and growth modification. However, the 1-year follow-up cephalometric study of Shetye et al[21] also showed that the midface has the capability of additional growth in a downward direction, even though those authors had used no devices for retention after LeFort III distraction with the rigid external distractor system. Additionally, the anteroposterior length of the anterior cranial base in our patient was increased by approximately 5 mm, which was in the normal range of Japanese male growth without syndromes, and this might compensate for any relapse after the maxillary advancement. It also suggests that craniofacial growth had been available even though the surgical procedure was performed at an early age. McCarthy et al[29] initially speculated that forward

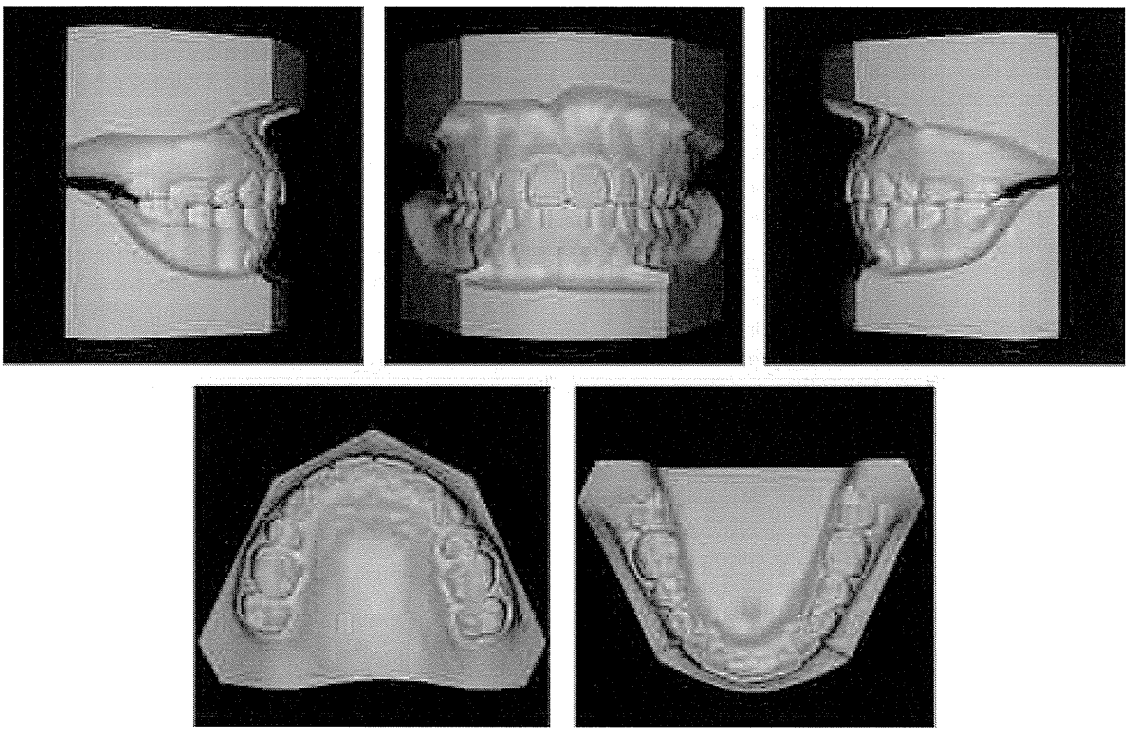

Fig 11. Posttreatment dental models.

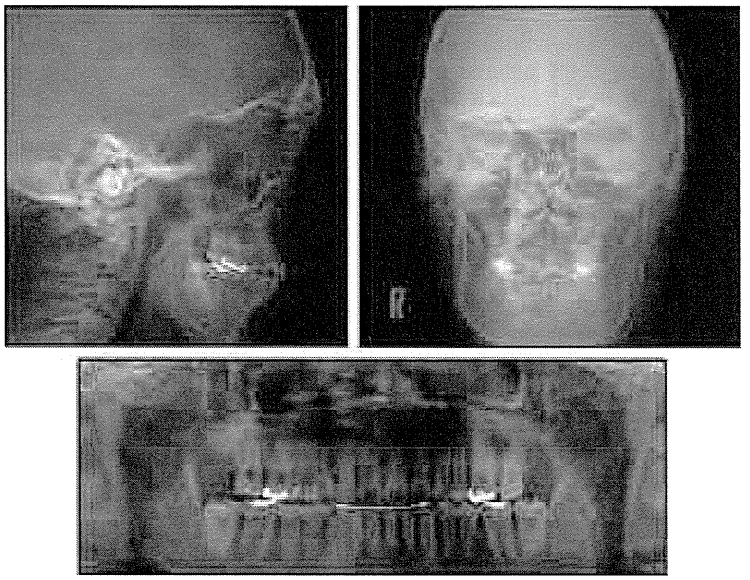

Fig 12. Posttreatment radiographs.

maxillary growth occurs in children with craniofacial dysostosis after LeFort III osteotomy. In addition, long-term follow-up studies of traditional LeFort III osteotomies showed a relatively stable postoperative position of the midface and also suggested that surgery does not negatively affect maxillary growth.[3-9] Furthermore, several reports indicated that relapse rates after distraction were lower than after conventional osteotomy because of good soft-tissue adaptations.[22,28,30-32] Our results indicate long-term stability after LeFort III distraction osteogenesis in a growing patient with Crouzon syndrome.

Several previous reports suggested a syndrome-specific mandibular malformation in Crouzon syndrome.[2,33,34] In our study, the ramus height was similar to the Japanese norm, but the mandibular body length was significantly shorter at the end of active treatment, since the increase of the mandibular body length during the 9 years of observation after distraction was small. These results correspond to the previous cephalometric studies of Crouzon syndrome.[2,34] This mandibular growth pattern might be convenient for compensation of relapse after maxillary advancement surgery, but it also could worsen the facial profile and the occlusion after the active growth phase. In addition, the long-term use of protraction headgear might cause undesirable counteractions such as extrusion of the maxillary posterior teeth and clockwise rotation of the mandible. As results of these phenomena, overbite was reduced, and the patient had a skeletal open-bite tendency with a steep mandibular plane angle. These syndrome-specific growth patterns and methodologically induced compensations should be considered in planning LeFort III distraction osteogenesis treatment in children with Crouzon syndrome.

The most outstanding advantage of early treatment in patients with a dentofacial deformity must be the improvement in their psychological development before adolescence. Moreover, early improvements of the functional disturbances should contribute to altering their succeeding growth pattern more favorably. In this patient, the airway obstruction was eliminated immediately after the LeFort III distraction, and adequate maxillofacial growth and long-term stability were observed. As the result of the distraction performed in the mixed dentition, the total treatment period became longer; however, the complex orthodontic treatment with multibracketed appliances could be finished in only 1 year. The complicated appliances usually become physical and psychological distresses for a patient. Therefore, we believe that the early treatment provided a meaningful outcome for this patient.

CONCLUSIONS

We reported the successful treatment of a patient with midfacial hypoplasia from Crouzon syndrome by LeFort III distraction using the rigid external distractor system in the mixed dentition. After distraction, acceptable facial growth was observed, and no relapse of the maxillary advancement was noted after 9 years. However, syndrome-specific growth and methodologically induced compensations should be considered when planning a LeFort III distraction osteogenesis in childhood for the treatment of a patient with Crouzon syndrome.

REFERENCES

1. Crouzon O. Dysostose cranio-faciale hereditair. Bull Mem Soc Med Hop Paris 1912;33:545-55.
2. Kreiborg S. Crouzon syndrome. A clinical and roentgencephalometric study. Scand J Plast Reconstr Surg Suppl 1981;18:1-198.
3. Epker BN, Wolford LM. Middle-third facial osteotomies: their use in the correction of congenital dentofacial and craniofacial deformities. J Oral Surg 1976;34:324-42.
4. Freihofer HP Jr. Results after midface-osteotomies. J Maxillofac Surg 1973;1:30-6.
5. Kaban LB, West B, Conover M, Will L, Mulliken JB, Murray JE. Midface position after Le Fort III advancement. Plast Reconstr Surg 1984;73:758-67.
6. Kaban LB, Conover M, Mulliken JB. Midface position after Le Fort III advancement: a long-term follow-up study. Cleft Palate J 1986;23(Suppl 1):75-7.
7. McCarthy JG, La Trenta GS, Breitbart AS, Grayson BH, Bookstein FL. The Le Fort III advancement osteotomy in the child under 7 years of age. Plast Reconstr Surg 1990;86:633-46.
8. Meazzini MC, Mazzoleni F, Caronni E, Bozzetti A. Le Fort III advancement osteotomy in the growing child affected by Crouzon's and Apert's syndromes: presurgical and postsurgical growth. J Craniofac Surg 2005;16:369-77.
9. Phillips JH, George AK, Tompson B. Le Fort III osteotomy or distraction osteogenesis imperfecta: your choice. Plast Reconstr Surg 2006;117:1255-60.
10. McCarthy JG, Schreiber J, Karp N, Thorne CH, Grayson BH. Lengthening the human mandible by gradual distraction. Plast Reconstr Surg 1992;8:1-8.
11. Cohen SR, Rutrick RE, Burstein FD. Distraction osteogenesis of the human craniofacial skeleton: initial experience with new distraction system. J Craniofac Surg 1995;6:368-74.
12. Polley JW, Figueroa AA. Management of severe maxillary deficiency in childhood and adolescence through distraction osteogenesis with an external, adjustable, rigid distraction device. J Craniofac Surg 1997;8:181-5.
13. Figueroa AA, Polley JW. Management of severe cleft maxillary deficiency with distraction osteogenesis: procedure and results. Am J Orthod Dentofacial Orthop 1999;115:1-12.
14. Krimmel M, Cornelius CP, Roser M, Bacher M, Reinert S. External distraction of the maxilla in patients with craniofacial dysplasia. J Craniofac Surg 2001;12:458-63.
15. Swennen G, Dujardin T, Goris A, De Mey A, Malevez C. Maxillary distraction osteogenesis: a method with skeletal anchorage. J Craniofac Surg 2000;11:120-7.

16. Kuroda S, Araki Y, Oya S, Mishima K, Sugawara T, Takano-Yamamoto T. Maxillary distraction osteogensis to treat maxillary hypoplasia: comparison of an internal and an external system. Am J Orthod Dentofacial Orthop 2005;127:493-8.
17. Cohen SR, Holmes RE. Internal Le Fort III distraction with biodegradable devices. J Craniofac Surg 2001;12:264-72.
18. Matsumoto K, Nakanishi H, Koizumi Y, Seike T, Okazaki M, Yokozeki M, et al. Segmental distraction of the midface in a patient with Crouzon syndrome. J Craniofac Surg 2002;13:273-8.
19. Satoh K, Mitsukawa N, Tosa Y, Kadomatsu K. Le Fort III midfacial distraction using an internal distraction device for syndromic craniosynostosis: device selection, problems, indications, and a proposal for use of a parallel bar for device-setting. J Craniofac Surg 2006;178:1050-8.
20. Meling TR, Hans-Erik H, Per S, Due-Tonnessen BJ. Le Fort III distraction osteogenesis in syndromal craniosynostosis. J Craniofac Surg 2006;17:28-39.
21. Shetye PR, Boutros S, Grayson BH, McCarthy JG. Midterm follow-up of midface distraction for syndromic craniosynostosis: a clinical and cephalometric study. Plast Reconstr Surg 2007;120:1621-32.
22. Fearon JA. Halo distraction of the Le Fort III in syndromic craniosynostosis: a long-term assessment. Plast Reconstr Surg 2005;115: 1524-36.
23. Wada K, Matsushita K, Shimazaki S, Miwa Y, Hasuike Y, Susami R. An evaluation of a new case analysis of a lateral cephalometric roentgenogram. J Kanazawa Med Univ 1981;6:60-70.
24. Nout E, Cesteleyn LL, van der Wal KG, van Adrichem LN, Mathijssen IM, Wolvius EB. Advancement of the midface, from conventional Le Fort III osteotomy to Le Fort III distraction: review of the literature. Int J Oral Maxillofac Surg 2008; 37:781-9.
25. Fearon JA. The Le Fort III osteotomy: to distract or not to distract? Plast Reconstr Surg 2001;107:1091-103.
26. Cedars MG, Linck DL 2nd, Chin M, Toth BA. Advancement of the midface using distraction techniques. Plast Reconstr Surg 1999; 103:429-41.
27. Chin M, Toth BA. Le Fort III advancement with gradual distraction using internal devices. Plast Reconstr Surg 1997;100:819-30.
28. Iannetti G, Fadda T, Agrillo A, Poladas G, Iannetti G, Filiaci F. Le-Fort III advancement with and without osteogenesis distraction. J Craniofac Surg 2006;17:536-43.
29. McCarthy JG, Grayson B, Bookstein F, Vickery C, Zide B. Le Fort III advancement osteotomy in the growing child. Plast Reconstr Surg 1984;74:343-54.
30. Gosain AK. Distraction osteogenesis of the craniofacial skeleton. Plast Reconstr Surg 2001;107:278-80.
31. McCarthy JG, Stelnicki EJ, Mehrara BJ, Longaker MT. Distraction osteogenesis of the craniofacial skeleton. Plast Reconstr Surg 2001;107:1812-27.
32. Wiltfang J, Hirschfelder U, Neukam FW, Kessler P. Long-term results of distraction osteogenesis of the maxilla and midface. Br J Oral Maxillofac Surg 2002;40:473-9.
33. Costaras-Volarich M, Pruzansky S. Is the mandible intrinsically different in Apert and Crouzon syndromes? Am J Orthod 1984;85: 475-87.
34. Boutros S, Shetye PR, Ghali S, Carter CR, McCarthy JG, Grayson BH. Morphology and growth of the mandible in Crouzon, Apert, and Pfeiffer syndromes. J Craniofac Surg 2007;18:146-50.

Congenital Anomalies
THE JAPANESE TERATOLOGY SOCIETY

82 *Congenital Anomalies* 2012; **52**, 82–86 doi:10.1111/j.1741-4520.2012.00356.x

ORIGINAL ARTICLE

Age-dependent change in behavioral feature in Rubinstein-Taybi syndrome

Tatsuhiko Yagihashi,[1,2] Kenjiro Kosaki,[3] Nobuhiko Okamoto,[5] Seiji Mizuno,[6] Kenji Kurosawa,[7] Takao Takahashi,[1] Yuji Sato[2], and Rika Kosaki[1,4]

[1]Department of Pediatrics, [2]Center for Clinical Research, [3]Center for Medical Genetics, Keio University School of Medicine, [4]Division of Clinical Genetics and Molecular Medicine, National Center for Child Health and Development, Tokyo, [5]Osaka Medical Center and Research Institute for Maternal and Child Health, Osaka, [6]Department of Pediatrics, Central Hospital, Aichi Human Service Center, Aichi, and [7]Department of Medical Genetics, Kanagawa Children's Hospital, Kanagawa, Japan

ABSTRACT **Rubinstein-Taybi syndrome (RTS) is characterized by developmental delay, postnatal growth retardation, typical facial appearance, and broad thumbs and big toes. The behavioral phenotype of children with RTS has been described as friendly and having good social contacts; however, a short attention span and hyperactivity are sometimes present. Little attention has been paid to the behavioral aspects of adults with RTS. We conducted an observational study focusing on behavioral problems in adolescents and adults with RTS compared with children with RTS. A total of 63 patients with RTS and their caretakers answered self-administered questionnaires regarding behavioral features including the Child Behavior Checklist (CBCL). High total CBCL scores were observed, and the mean score was beyond the clinical cut-off point. After stratification into two groups according to age, the older group (≥14 years) displayed statistically significant higher scores for *Anxious/Depression* ($P = 0.002$) and *Aggressive Behavior* ($P = 0.036$) than the younger group (≤13 years). In analyses of single items, statistically significant differences between the younger group and the older group were found for 'Nervous, high-strung, or tense' (31.3% vs 67.7%, $P = 0.004$) and 'Too fearful or anxious' (37.5% vs 64.5%, $P = 0.032$). Here, we showed that the specific behavioral phenotypes of RTS change during adolescence, with anxiety, mood instability, and aggressive behavior emerging as patients age. A clear need exists to follow-up patients with RTS to catch the eventual emergence of psychiatric problems with age. If necessary, pharmacological treatment should be considered.**

Key Words: age-dependent change, behavioral problem, Child Behavior Checklist, depression, Rubinstein-Taybi syndrome

INTRODUCTION

Rubinstein-Taybi syndrome (RTS; OMIM 180849) is characterized by developmental delay, postnatal growth retardation, microcephaly, typical facial appearance, and broad thumbs and big toes (Rubinstein and Taybi 1963). Chromosomal or molecular abnormalities are found in about 55% of cases (Hennekam 2006; Stef et al. 2007). Its occurrence is generally sporadic, and the condition can be caused by a micro-deletion of chromosome 16p13.3 or by a mutation in either the gene encoding the transcriptional coactivator CREB-binding protein (CREBBP) on chromosome 16p13 or the EP300 gene on chromosome 22q13 (Bartsch et al. 2010). The diagnosis of RTS, however, remains primarily clinical.

In the original report by Rubinstein and Taybi (1963), the behavioral phenotype of RTS was described as hyperactivity and emotional lability. Later studies demonstrated that children with RTS were generally friendly and more readily accepted social contacts; however, RTS children sometimes have irritability and impulsivity (Gotts and Liemohn 1977; Stevens et al. 1990). The first epidemiological study to use a standardized psychometric tool, the Child Behavior Checklist (CBCL), focused on the psychological aspects of RTS. It showed that the most frequently reported behavioral problems were 'acts too young for age', 'can't concentrate', 'poorly coordinated, clumsy', and 'likes to be alone' (Hennekam et al. 1992). A recent comparative study between children with RTS and a control group concluded that a short attention span, stereotypical behavior, and poor coordination were common behavioral features in RTS (Galera et al. 2009).

There is emerging evidence that RTS may be associated with specific behavioral problems; however, little attention has been paid to the behavioral aspects of adults with RTS. Levitas and Reid (1998) performed psychiatric evaluations of adults with RTS who had been referred for behavioral problems. The resulting diagnoses were clustered into mood disorders and obsessive-compulsive disorder spectrum. Similarly, a case report described a 39-year-old woman who presented with symptoms of severe hyperactivity, short attention span, mood instability, and aggressive outbursts in a cyclical pattern (Hellings et al. 2002). Verhoeven et al. (2010) also reported another adult patient with RTS who was admitted because of depressive mood, impulsivity, and temper outbursts. Hennekam (2006) reported that short attention span, stubbornness, lack of persistence, and emotional lability became increasingly apparent during early adulthood, leading to uncertain behavior and occasional aggressiveness. These reports in adult patients support a potential link between RTS and mood instability/aggressive behavior. Whether a specific age-dependent behavioral pattern of RTS exists remains to be determined using a standardized psychometric tool. Here, we report an observational study focusing on behavioral problems in adolescents and adults with RTS, compared with children with RTS.

MATERIALS AND METHODS

Patients

Patients with RTS were recruited from the Rubinstein-Taybi Syndrome Family Support Group, Japan (Cosmos). This nationwide

Correspondence: Rika Kosaki, MD, Division of Clinical Genetics and Molecular Medicine, National Center for Child Health and Development, 2-10-1 Okura, Setagaya-ku, Tokyo, Japan. Email: kosaki-r@ncchd.go.jp
Received November 28, 2011; revised and accepted January 9, 2012.

organization was formed in 1994 by and for families of individuals with RTS and presently includes about 100 family members. Inclusion in the present study required a confirmed diagnosis of RTS made by clinical geneticists based on the presence of diagnosis criteria, including abnormalities of the face, broad and angulated thumbs and big toes, growth retardation, and mental retardation. Molecular tests for the diagnosis of RTS were not required.

Study design

A postal questionnaire was sent in December 2010 to all individuals on the mailing list of the Rubinstein-Taybi Syndrome Family Support Group, Japan. The consent form and questionnaires were sent with a return envelope to each participant. They were invited to complete the self-administered questionnaires regarding the socio-behavioral features of their children, including the Child Behavior Checklist, and to return the forms to our hospital. The Ethics Committee at Keio University approved the study protocol.

Child Behavior Checklist (CBCL)

The CBCL is composed of questions related to a total of 113 items categorized into the following eight subscale items: (I) *Withdrawn*; (II) *Somatic Complaints*; (III) *Anxious/Depressed*; (IV) *Social Problems*; (V) *Thought Problems*; (VI) *Attention Problems*; (VII) *Delinquent Behavior*; and (VIII) *Aggressive Behavior*. *Internalizing* (I + II + III), *Externalizing* (VII + VIII), and *Total Problems* were also derived from these subscales. Caretakers answered each question by selecting one of three answer choices. The raw scores for 11 scales were calculated from the scores for the answers. Then, the raw scores were converted into T-scores according to the profile sheet based on a normal Japanese population (Achenbach 1991; Itani et al. 2001). In this study, the T-scores of patients aged under 4 years and over 15 years were estimated according to the standard profile of 4–11 years and 12–15 years, respectively. Previously, a higher score was found to be associated with a greater likelihood of problematic behavior for that scale (Achenbach 1991). A T-score > 63 in *Total Problems* and T-score > 67 in each subscale suggested that the patient should have some clinical problems.

Data analyses

The distributions of sex, age, presence or absence of genetic abnormalities, and CBCL scores were examined for all the subjects. The patients were then stratified according to age into two groups. Patients younger than the 50%tile (≤13 years) were classified as the younger group, and those who were older (≥14 years) were classified as the older group. We compared the T-scores for the 11 scales that were examined between the two groups (Mann-Whitney *U*-test). We also compared the two groups for the single items. For these single items and to assess clinically relevant problems, we constructed dichotomous dependent variables by considering a rating of 0 as 'No' versus a rating of 1 or 2 as 'Yes'. To examine a possible gene-behavior link, we finally compared the T-scores between the two age groups only in subjects with genetic abnormalities associated with RTS. An alpha level of 0.05 (two-tailed) was adopted as the criterion for statistical significance. Statistical analyses were performed using SPSS version 17.0 (SPSS Inc, Chicago, IL, USA).

RESULTS

Background of the subjects

A total of 63 patients (37 men and 26 women), aged 1–38 years (median: 13 years) were studied. Molecular tests had been performed in 20 of 63 patients (32%). Molecular abnormalities (i.e. intragenic mutations or deletions in CREBBP or EP300 gene), had been identified in nine of 20 patients (45%). The mean T-scores were 63.5 for *Total Problems*, 57.2 for *Internalizing*, 56.1 for *Externalizing*, 58.1 for *Withdrawn*, 57.9 for *Somatic Complaints*, 56.6 for *Anxious/Depression*, 67.3 for *Social Problems*, 62.1 for *Thought Problems*, 67.1 for *Attention Problems*, 57.8 for *Delinquent Behavior*, and 56.1 for *Aggressive Behavior*. The T-score for *Total Problems* was beyond the clinical cut-off point of 63. Questions that were answered 'Yes' by more than 70% of patients included 'Acts too young for his/her age' (97%), 'Can't concentrate, can't pay attention for long' (92%), 'Poorly coordinated or clumsy' (87%), and 'Clings to adults or too dependent' (71%).

CBCL scores after stratification according to age

Figure 1 shows mean CBCL scale scores among subjects with RTS after stratification according to interquartile age (≤7, 8–13, 14–22, and ≥23 years). The mean *Total Problem* score in each group was 62, 63, 65, and 64, respectively. The scores for the three groups aged 8 years or older exceeded the cut-off value of 63 points. Two CBCL scales, *Social Problems*, and *Attention Problems*, were beyond the cut-off point of 67 in all the age groups. The scores for *Anxious/Depression* and *Aggressive Behavior* tended to increase with age (Fig. 1). After stratification into two groups according to age, the older group (≥14 years) displayed statistically significant higher scores of *Anxious/Depression* ($P = 0.002$) and *Aggressive Behavior* ($P = 0.036$) than the younger group (≤13 years) (Table 1a). Among nine subjects with identified genetic abnormalities, the older group tended to display higher scores for *Anxious/Depression* ($P = 0.037$) and *Aggressive Behavior* ($P = 0.157$) than the younger group (Table 1b). In analyses of single items, statistically significant differences between the younger group and the older group were found for 'Nervous, high-strung, or tense' (31.3% vs 67.7%, $P = 0.004$), 'Can't concentrate, can't pay attention for long' (84.4% vs 100.0%, $P = 0.022$), and 'Too fearful or anxious' (37.5% vs 64.5%, $P = 0.032$) (Table 2).

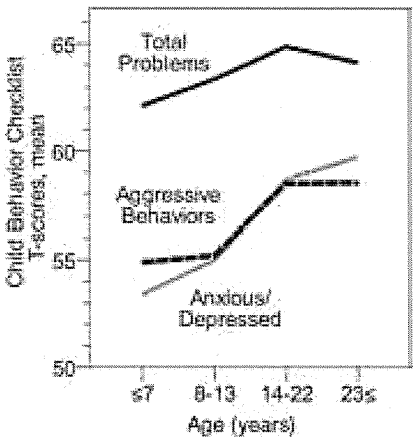

Fig. 1 Temporal scores for the Child Behavior Checklist scales in subjects with Rubinstein-Taybi syndrome. Line charts represent mean scores for CBCL scales in each age group. T-score, standardized score calculated from the raw score for each subject based on a normal population. Black solid line, *Total Problems*; grey solid line, *Anxious/Depressed*; dotted line: *Aggressive Behaviors*.

Table 1 T-scores for Child Behavior Checklist (CBCL) compared between younger and older groups with Rubinstein-Taybi syndrome

CBCL T-scores, median (interquartile range)	Younger group N = 32	Older group N = 31	*P*-value
All subjects (63 subjects)			
Total problems	63.0 (57.0–68.0)	64.0 (61.0–68.0)	0.268
Internalizing	57.0 (50.5–61.0)	61.0 (54.0–64.0)	0.072
Externalizing	54.0 (47.0–60.0)	57.0 (54.0–61.0)	0.069
Withdrawn	56.0 (53.0–63.0)	59.0 (50.0–63.0)	0.878
Somatic complaints	55.0 (50.0–67.0)	54.0 (54.0–64.0)	0.972
Anxious/depressed	52.0 (50.0–56.5)	60.0 (52.0–63.0)	0.002*
Social problems	65.0 (63.0–69.0)	68.0 (65.0–70.0)	0.150
Thought problems	62.5 (50.0–73.0)	56.0 (50.0–73.0)	0.829
Attention problems	69.0 (62.0–72.0)	67.0 (63.0–70.0)	0.756
Delinquent behavior	54.5 (52.0–65.0)	55.0 (50.0–63.0)	0.878
Aggressive behavior	52.5 (50.0–58.5)	57.0 (51.0–61.0)	0.036*
CBCL T-scores, median (interquartile range)	Younger group N = 5	Older group N = 4	*P*-value
Subjects with genetic abnormalities (9 subjects)			
Total problems	63.0 (61.0–66.0)	66.0 (63.0–69.5)	0.389
Internalizing	61.0 (56.0–61.0)	59.5 (56.5–63.0)	0.701
Externalizing	51.0 (48.0–57.0)	59.5 (54.5–62.0)	0.176
Withdrawn	53.0 (53.0–59.0)	62.0 (56.0–64.0)	0.385
Somatic complaints	67.0 (55.0–67.0)	57.0 (50.0–65.0)	0.211
Anxious/depressed	52.0 (52.0–58.0)	59.0 (58.0–61.5)	0.037*
Social problems	63.0 (63.0–70.0)	70.0 (68.0–71.5)	0.118
Thought problems	69.0 (56.0–70.0)	72.5 (60.0–76.5)	0.385
Attention problems	69.0 (67.0–69.0)	67.0 (65.0–74.0)	0.802
Delinquent behavior	65.0 (54.0–65.0)	55.0 (55.0–60.5)	0.800
Aggressive behavior	50.0 (50.0–54.0)	59.0 (53.5–61.0)	0.157

*$P < 0.05$ (Mann–Whitney *U*-test).
T-score, standardized score calculated from raw score of each subject based on a normal population.
Younger group, subjects aged <13 years; Older group, subjects aged >14 years.

DISCUSSION

Here, we showed that the specific behavioral phenotype of RTS changes during adolescence, with anxiety, depression, and aggressive behaviors emerging at that time. The present study represents the first comprehensive assessment of age-dependent changes in behavior using a standardized psychometric tool, the CBCL, and reinforces the observations of previous case reports or case series describing the emergence of nervousness, anxiety, stubbornness, sullenness, and irritability during adolescence or adulthood (Levitas and Reid 1998; Hellings et al. 2002; Verhoeven et al. 2010).

As demonstrated in studies of other congenital malformation syndromes, including Costello syndrome and 22q11.2 deletion syndrome (Galera et al. 2006; Jansen et al. 2007), the CBCL has been instrumental in delineating disease-specific behavioral patterns. However, a limitation of this study is the use of the CBCL in adults, because the T-score of the CBCL Japanese version was standardized only between 4- and 15-year-old children but not at older ages (Itani et al. 2001). More refined evaluations (e.g. standardized diagnostic interviews) are needed to confirm the diagnostic criteria of psychiatric diseases in the adolescent and adult patients. Furthermore, a close longitudinal follow-up of patients with RTS would clarify whether behavioral problems, including mood instability or temper tantrums, need subsequent psychiatric management (e.g. drug treatment with mood stabilizers).

The reason why these psychiatric traits arise during adolescence is unknown at present, although postnatal dysfunction of the CREBBP/EP300 genes in patients with RTS has been postulated to lead to neural alterations during adolescence (Alarcon et al. 2004; Hennekam 2006). Cyclic adenosine monophosphate response element binding protein (CREB) and its cofactor, CREBBP, regulates the expression of many genes involved in the development of the nervous system, learning, memory and cell survival (Viola et al. 2000; Hardingham et al. 2001; Lonze and Ginty 2002). The observations that the CREB protein expressions were significantly decreased in patients with depression speak towards CREB and CREBBP's potential involvement in the pathophysiology of psychiatric diseases (Yuan et al. 2010; Ren et al. 2011). These observations postulate that postnatal dysfunction of the CREBBP/EP300 genes in patients with RTS may play an important role in the

Table 2 Common behaviors compared between younger and older groups with Rubinstein-Taybi syndrome (N = 63)

CBCL single items, number (%)	Younger group N = 32		Older group N = 31		*P*-value
Nervous, high-strung, or tense	10	31.3%	21	67.7%	0.004**
Wets the bed	21	65.6%	9	29.0%	0.004**
Can't concentrate, can't pay attention for long	27	84.4%	31	100.0%	0.022*
Bowel movements outside toilet	18	56.3%	9	29.0%	0.029*
Doesn't seem to feel guilty after misbehaving	18	56.3%	9	29.0%	0.029*
Too fearful or anxious	12	37.5%	20	64.5%	0.032*
Can't sit still, restless, or hyperactive	20	62.5%	12	38.7%	0.059
Can't get his/her mind off certain thoughts; obsessions	5	15.6%	11	35.5%	0.070
Stubborn, sullen, or irritable	11	34.4%	17	54.8%	0.102
Poorly coordinated or clumsy	26	81.3%	29	93.5%	0.143
Acts too young for his/her age	32	100.0%	29	93.5%	0.144

*$P < 0.05$ (Mann–Whitney *U*-test); **$P < 0.01$ (Mann–Whitney *U*-test).
Younger group, subjects aged <13 years; Older group, subjects aged >14 years.

pathophysiology of subsequent behavioral features in RTS and that biological pathway mediated by CREB may well be an important target when pharmacological intervention is to be explored. Several different mouse models of RTS have been created in which CBP or p300 function is genetically altered, and these mutant mice exhibit deficits in synaptic plasticity and memory (Alarcon et al. 2004; Korzus et al. 2004). In addition, these studies have suggested that some of the cognitive deficits observed in individuals with RTS may not simply be due to the reduction of CBP during development but might also result from the continued requirement of specific enzymatic activities throughout life, as some deficits observed in CBP-mutant mice can be ameliorated using inhibitors of enzymes that compensate for a reduction in the functioning of CBP as a CREB co-activator, such as histone deacetylase inhibitors (HDACI) (Alarcon et al. 2004; Korzus et al. 2004).

These animal findings may open the possibility of pharmacological treatment using HDACI for the neurological deficits observed in RTS patients, enabling normal CBP function to be reestablished and alleviating some of their symptoms. In support of this hypothesis, a previous report has described an adult patient with RTS who was successfully treated with valproic acid: valproic acid is an antiepileptic drug that acts as a clinically available HDACI and is already established as a mood stabilizers to alleviate certain psychiatric symptoms such as mood instability, irritability, and aggressiveness even in the absence of seizures (Hellings et al. 2002; Abel and Zukin 2008). If further case reports are accumulated in the future, it may be worthwhile to test the effectiveness of HDACIs as disease-modifying drugs, which are used to modify the natural course of the disease, rather than curing the disease itself. These drugs might not be a cure for RTS, but they can reduce the deteriorations in cognitive deficits and subsequent psychiatric problems.

In summary, we found that the specific behavioral phenotype of RTS changes during adolescence in an age-dependent manner. Anxiety, mood instability, and aggressive behavior tended to emerge as individuals with RTS aged. There is a clear need to follow up patients with RTS to catch the eventual emergence of psychiatric problems with age. If necessary, patients with RTS should be referred to a psychiatrist and pharmacological treatment should be considered.

ACKNOWLEDGMENTS

We thank the families of the Rubinstein-Taybi Syndrome Family Support Group, Japan (Cosmos) for participating in this study. We also thank the Contract grant sponsor: The Ministry of Health, Labour, and Welfare of Japan.

REFERENCES

Abel T, Zukin RS. 2008. Epigenetic targets of HDAC inhibition in neurodegenerative and psychiatric disorders. Curr Opin Pharmacol 8:57–64.

Achenbach TM. 1991. Manual for the Child Behavior Checklist 4–18 and 1991 profile. Burlington, VT: University of Vermont, Department of Psychiatry.

Alarcon JM, Malleret G, Touzani K et al. 2004. Chromatin acetylation, memory, and LTP are impaired in CBP+/- mice: a model for the cognitive deficit in Rubinstein-Taybi syndrome and its amelioration. Neuron 42:947–959.

Bartsch O, Kress W, Kempf O, Lechno S, Haaf T, Zechner U. 2010. Inheritance and variable expression in Rubinstein-Taybi syndrome. Am J Med Genet A 152A:2254–2261.

Galera C, Delrue MA, Goizet C et al. 2006. Behavioral and temperamental features of children with Costello syndrome. Am J Med Genet A 140:968–974.

Galera C, Taupiac E, Fraisse S et al. 2009. Socio-behavioral characteristics of children with Rubinstein-Taybi syndrome. J Autism Dev Disord 39:1252–1260.

Gotts EE, Liemohn WP. 1977. Behavioral characteristics of three children with the broad thumb-hallux (Rubinstein-Taybi) syndrome. Biol Psychiatry 12:413–423.

Hardingham GE, Arnold FJ, Bading H. 2001. Nuclear calcium signaling controls CREB-mediated gene expression triggered by synaptic activity. Nat Neurosci 4:261–267.

Hellings JA, Hossain S, Martin JK, Baratang RR. 2002. Psychopathology, GABA, and the Rubinstein-Taybi syndrome: a review and case study. Am J Med Genet 114:190–195.

Hennekam RC. 2006. Rubinstein-Taybi syndrome. Eur J Hum Genet 14:981–985.

Hennekam RC, Baselier AC, Beyaert E et al. 1992. Psychological and speech studies in Rubinstein-Taybi syndrome. Am J Ment Retard 96:645–660.

Itani T, Kanbayashi Y, Nakata Y et al. 2001. Study on validity of the Japanese version of CBCL/4-18.]. Shyoni No Seishin To Shinkei 4:243–252. (In Japanese.)
Jansen PW, Duijff SN, Beemer FA et al. 2007. Behavioral problems in relation to intelligence in children with 22q11.2 deletion syndrome: a matched control study. Am J Med Genet A 143:574–580.
Korzus E, Rosenfeld MG, Mayford M. 2004. CBP histone acetyltransferase activity is a critical component of memory consolidation. Neuron 42:961–972.
Levitas AS, Reid CS. 1998. Rubinstein-Taybi syndrome and psychiatric disorders. J Intellect Disabil Res 42:(Pt 4): 284–292.
Lonze BE, Ginty DD. 2002. Function and regulation of CREB family transcription factors in the nervous system. Neuron 35:605–623.
Ren X, Dwivedi Y, Mondal AC, Pandey GN. 2011. Cyclic-AMP response element binding protein (CREB) in the neutrophils of depressed patients. Psychiatry Res 185:108–112.
Rubinstein JH, Taybi H. 1963. Broad thumbs and toes and facial abnormalities. A possible mental retardation syndrome. Am J Dis Child 105:588–608.
Stef M, Simon D, Mardirossian B et al. 2007. Spectrum of CREBBP gene dosage anomalies in Rubinstein-Taybi syndrome patients. Eur J Hum Genet 15:843–847.
Stevens CA, Carey JC, Blackburn BL. 1990. Rubinstein-Taybi syndrome: a natural history study. Am J Med Genet Suppl 6:30–37.
Verhoeven WM, Tuinier S, Kuijpers HJ, Egger JI, Brunner HG. 2010. Psychiatric profile in rubinstein-taybi syndrome. A review and case report. Psychopathology 43:63–68.
Viola H, Furman M, Izquierdo LA et al. 2000. Phosphorylated cAMP response element-binding protein as a molecular marker of memory processing in rat hippocampus: effect of novelty. J Neurosci 20:RC112.
Yuan P, Zhou R, Wang Y et al. 2010. Altered levels of extracellular signal-regulated kinase signaling proteins in postmortem frontal cortex of individuals with mood disorders and schizophrenia. J Affect Disord 124:164–169.

RESEARCH LETTER

AMERICAN JOURNAL OF medical genetics PART A

Monozygotic Twins of Rubinstein–Taybi Syndrome Discordant for Glaucoma

Rika Kosaki,[1]* Hideki Fujita,[1] Hazuki Takada,[1] Michiyo Okada,[1] Chiharu Torii,[2] and Kenjiro Kosaki[2]

[1]Division of Medical Genetics, National Center for Child Health and Development, Tokyo, Japan

[2]Department of Pediatrics, Keio University School of Medicine, Tokyo, Japan

Received 15 December 2010; Accepted 3 February 2011

TO THE EDITOR:

Rubinstein–Taybi syndrome (RTS) is characterized by broad thumbs and toes, downward slanted palpebral fissures, a prominent nose with the nasal septum extending below the alae nasi, a hypoplastic maxilla with a narrow plate, thick eyebrows, long eyelashes, a short stature, and moderate intellectual disability [Hennekam, 2006]; its incidence is estimated to be 1 in 100,000. Most cases are sporadic, and about half of all cases have a heterozygous mutation in the *CREBBP* gene; rare cases have a heterozygous *EP300* mutation. Both genes encode histone acetyltransferases (HAT), which are transcriptional co-activators that play critical roles in epigenetic regulation through histone acetylation [Roelfsema and Peters, 2007]. Among the more than 600 cases of RTS reported to date, at least 11 sets of monozygotic twins [Pfeifer, 1968; Gorlin et al., 1976; Schinzel et al., 1979; Kajii et al., 1981; Baraitser and Preece, 1983; Widd, 1983; Ghanem and Dawod, 1990; Hennekam et al., 1990; Robinson et al., 1993; Preis and Majewski, 1995] have been documented.

Here, we present monozygotic twins concordant for the RTS phenotype. The monozygosity and RTS diagnosis were both confirmed using molecular methods. Interestingly, the twins were concordant for facial and limb features but were discordant for body size and the presence of congenital glaucoma. The discordance in the former characteristic (i.e., the body size) was ascribed to a twin-to-twin transfusion between the twins, whereas the discordance in the latter characteristic (i.e., the glaucoma) could not be explained.

The male twins were born to a 24-year-old Japanese G1P1-2 woman with no previous medical problems. Consanguinity or a family history of mental retardation was not present. The placentation was diamniotic and monochorionic. The pregnancy was remarkable for the disproportionate growth of the twins. An ultrasonographic diagnosis of twin-to-twin transfusion syndrome was made, and the vascular connection on the placenta between the twins was successfully disconnected using laser ablation.

The twins were delivered at 30 weeks of gestation. At birth, the weight of Twin A was 1,174 g and his length was 36 cm whereas the birth weight of Twin B was 960 g and his length was 34.5 cm. The postnatal courses of the twins were similar. Developmental delays were apparent: the twins were able to hold their heads up at 10 months, to sit alone at around 18 months, to walk alone at 3–1/2 years, and to speak meaningful words at 7 years.

How to Cite this Article:
Kosaki R, Fujita H, Takada H, Okada M, Torii C, Kosaki K. 2011. Monozygotic twins of Rubinstein–Taybi syndrome discordant for glaucoma.
Am J Med Genet Part A 155:1189–1191.

At the age of 16 months, the twins were referred to our genetic department because of developmental delays. Dysmorphic features (Fig. 1), which were all concordant between the twins, included broad thumbs and toe, downward slanting pleural fissures, a hypoplastic maxilla, a prominent nose with the nasal septum extending below the alae nasi, heavy eyebrows and long eyelashes, salmon patches, undescended testes, patent ductus arterious and a hearing impairment. However, only Twin A had bilateral congenital glaucoma and lens dislocations. A genotyping analysis using nine microsatellite markers (ALAS2, DXS1236, D7S527, D7S630, D9S1779, D9S15, D10S595, D10S2454, and D17S1705) confirmed the monozygosity of the twins. Chromosome analyses revealed normal karyotypes. Molecular screening of the *CREBBP* gene using denaturing high-performance liquid chromatography (DHPLC) was negative [Udaka et al., 2005].

Array comparative genomic hybridization using the Agilent 180K format CGH array designed by the International Standards for Cytogenomic Arrays Consortium (backbone resolution of 35 or 25 kb and 500 targeted regions including telomeres, centromeres, microdeletion/duplication regions, and X-linked mental retarda-

Grant sponsor: The Ministry of Health, Labour, and Welfare of Japan.
*Correspondence to:
Rika Kosaki, M.D., Division of Medical Genetics, National Center for Child Health and Development, 2-10-1 Okura, Setagaya-ku, Tokyo 157-8535, Japan. E-mail: kosaki-r@ncchd.go.jp
Published online 7 April 2011 in Wiley Online Library (wileyonlinelibrary.com).
DOI 10.1002/ajmg.a.33967

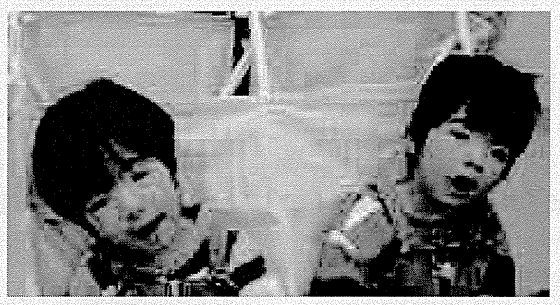

FIG. 1. Facial features of monozygotic twins with Rubinstein–Taybi syndrome (left: Twin A and right: Twin B).

tion genes) revealed a loss in the copy number for the 16p13.3 region (Fig. 2). The size of the deletion was 210 kb, extending from 3,810,524 to 4,0233,361 on 16p13.3 (hg18; NCBI Build 36.1). Genes within the deleted region included the 5′ half of the *CREBBP* locus and its adjacent *ADCV9* locus. We further compared the genomic DNA of Twin A and Twin B using the array, but no copy number differences were detected.

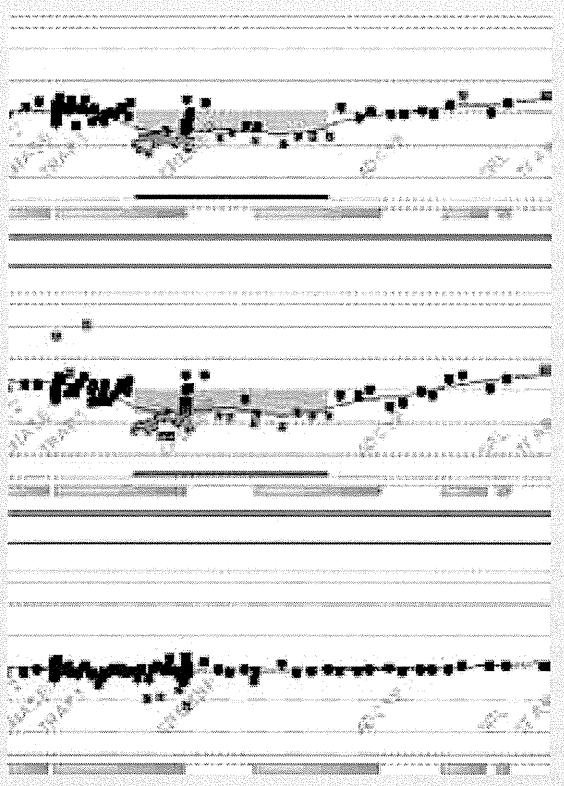

FIG. 2. Result of CGH array analysis (top: Twin A vs. control; middle: Twin B vs. control; bottom: Twin A vs. Twin B). The CGH array analysis revealed a 210 kb interstitial deletion of 16p13.3 involving *CREBBP* gene (top: gray area; middle: blue area).

Here, we document a case of monozygotic twins concordant for the RTS phenotype. To our knowledge, this twin pair represents the first twins whose monozygosity and RTS diagnosis have been confirmed using molecular methods. The monozygosity and diagnosis of several twin pairs with genetically determined multiple congenital anomaly syndromes have been reported including those with Smith–Magenis syndrome [Kosaki et al., 2007], Crouzon syndrome, Alagille syndrome, Sotos syndrome, and 22q11.2 deletion syndrome. RTS can now be added to this list.

The twins had concordant facial and limb features but were discordant for the presence of congenital glaucoma. Three potential mechanisms are capable of explaining this discordance: first, the glaucoma phenotype may not be causally related to the deletion of the RTS locus and may have appeared by chance as a polygenetic trait [Libby et al., 2005]. However, the occasional documentation of glaucoma in other RTS cases [Hennekam, 2006] suggests that the glaucoma phenotype is likely to be associated with the RTS deletion. Second, only Twin A might have experienced a "second hit" in a genomic region(s) other than chromosome 16p. Indeed, array CGH genomic studies of monozygotic twin genomes have revealed occasional differences in copy numbers [Bruder et al., 2008]. However, we did not detect such differences in the presently reported twins (data not shown). Thirdly, the discordance in the severities of the twin pairs could be ascribed to chance-like variations in the pathogenetic actions of the mutated gene. Intriguingly, epigenetic regulation plays a critical role in the stochastic nature of embryonic development, and *CREBBP*, the causative gene in the presently reported twins, represents an epigenetic regulator of embryogenesis [Robinson et al., 1993]. Indeed, a previously reported difference in the neurodevelopment of twins with RTS may support such a notion [Pfeifer, 1968; Buchinger and Stroder, 1973; Preis and Majewski, 1995].

REFERENCES

Baraitser M, Preece MA. 1983. The Rubinstein–Taybi syndrome: Occurrence in two sets of identical twins. Clin Genet 23:318–320.

Bruder CE, Piotrowski A, Gijsbers AA, Andersson R, Erickson S, Diaz de Stahl T, Menzel U, Sandgren J, von Tell D, Poplawski A, Crowley M, Crasto C, Partridge EC, Tiwari H, Allison DB, Komorowski J, van Ommen GJ, Boomsma DI, Pedersen NL, den Dunnen JT, Wirdefeldt K, Dumanski JP. 2008. Phenotypically concordant and discordant monozygotic twins display different DNA copy-number-variation profiles. Am J Hum Genet 82:763–771.

Buchinger G, Stroder J. 1973. Rubinstein–Taybi syndrome of probably monocygotic twins and 3 other children. Klin Padiatr 185:296–307.

Ghanem Q, Dawod S. 1990. Monozygotic twins concordant for Rubinstein–Taybi syndrome. Clin Genet 37:429–434.

Gorlin RJ, Pindborg JJ, Cohen MM. 1976. Rubinstein–Taybi syndrome. In: Gorlin RJ, Pindborg JJ, Cohen MM, editors. Syndromes of the Head and Neck, 2e. New York: McGraw Hill, Inc. pp 657–660.

Hennekam RC. 2006. Rubinstein–Taybi syndrome. Eur J Hum Genet 14:981–985.

Hennekam RC, Stevens CA, Van de Kamp JJ. 1990. Etiology and recurrence risk in Rubinstein–Taybi syndrome. Am J Med Genet Suppl 6:56–64.

Kajii T, Hagiwara K, Tsukahara M, Nakajima H, Fukuda Y. 1981. Monozygotic twins discordant for Rubinstein–Taybi syndrome. J Med Genet 18:312–314.

Kosaki R, Okuyama T, Tanaka T, Migita O, Kosaki K. 2007. Monozygotic twins of Smith–Magenis syndrome. Am J Med Genet Part A 143A: 768–769.

Libby RT, Gould DB, Anderson MG, John SW. 2005. Complex genetics of glaucoma susceptibility. Annu Rev Genomics Hum Genet 6:15–44.

Pfeifer RA. 1968. Rubinstein–Taybi syndrome in probably monozygotic twins. Humangenetik 6:84–87.

Preis S, Majewski F. 1995. Monozygotic twins concordant for Rubinstein–Taybi syndrome: Changing phenotype during infancy. Clin Genet 48:72–75.

Robinson TW, Stewart DL, Hersh JH. 1993. Monozygotic twins concordant for Rubinstein–Taybi syndrome and implications for genetic counseling. Am J Med Genet 45:671–673.

Roelfsema JH, Peters DJ. 2007. Rubinstein–Taybi syndrome: Clinical and molecular overview. Expert Rev Mol Med 9:1–16.

Schinzel AA, Smith DW, Miller JR. 1979. Monozygotic twinning and structural defects. J Pediatr 95:921–930.

Udaka T, Samejima H, Kosaki R, Kurosawa K, Okamoto N, Mizuno S, Makita Y, Numabe H, Toral JF, Takahashi T, Kosaki K. 2005. Comprehensive screening of CREB-binding protein gene mutations among patients with Rubinstein–Taybi syndrome using denaturing high-performance liquid chromatography. Congenit Anom (Kyoto) 45:125–131.

Widd S. 1983. Rubinstein–Taybi syndrome. Nurse Times 79:61–65.

Human Molecular Genetics, 2011, Vol. 20, No. 10 **2058–2070**
doi:10.1093/hmg/ddr090
Advance Access published on March 9, 2011

Insufficiency of BUBR1, a mitotic spindle checkpoint regulator, causes impaired ciliogenesis in vertebrates

Tatsuo Miyamoto[1], Sean Porazinski[2], Huijia Wang[2], Antonia Borovina[3,4], Brian Ciruna[3,4], Atsushi Shimizu[5], Tadashi Kajii[6], Akira Kikuchi[7], Makoto Furutani-Seiki[2] and Shinya Matsuura[1,*]

[1]Department of Genetics and Cell Biology, Research Institute for Radiation Biology and Medicine, Hiroshima University, Hiroshima 734-8553, Japan, [2]Centre for Regenerative Medicine, Department of Biology and Biochemistry, University of Bath, Bath BA2 7AY, UK, [3]Program in Developmental & Stem Cell Biology, The Hospital for Sick Children, Toronto, Ontario, Canada M5G 1X8, [4]Department of Molecular Genetics, University of Toronto, Toronto, Ontario, Canada M5S 1A8, [5]Department of Molecular Biology, Keio University School of Medicine, 35 Shinanomachi, Shinjuku-ku, Tokyo 160-8582, Japan, [6]Hachioji, Tokyo 192-0023, Japan and [7]Department of Molecular Biology and Biochemistry, Graduate School of Medicine, Osaka University, Osaka 565-0870, Japan

Received November 25, 2010; Revised and Accepted February 28, 2011

Budding uninhibited by benzimidazole-related 1 (BUBR1) is a central molecule of the spindle assembly checkpoint. Germline mutations in the budding uninhibited by benzimidazoles 1 homolog beta gene encoding BUBR1 cause premature chromatid separation (mosaic variegated aneuploidy) [PCS (MVA)] syndrome, which is characterized by constitutional aneuploidy and a high risk of childhood cancer. Patients with the syndrome often develop Dandy–Walker complex and polycystic kidneys; implying a critical role of BUBR1 in morphogenesis. However, little is known about the function of BUBR1 other than mitotic control. Here, we report that BUBR1 is essential for the primary cilium formation, and that the PCS (MVA) syndrome is thus a novel ciliopathy. Morpholino knockdown of *bubr1* in medaka fish also caused ciliary dysfunction characterized by defects in cerebellar development and perturbed left–right asymmetry of the embryo. Biochemical analyses demonstrated that BUBR1 is required for ubiquitin-mediated proteasomal degradation of cell division cycle protein 20 in the G0 phase and maintains anaphase-promoting complex/cyclosome-CDC20 homolog 1 activity that regulates the optimal level of dishevelled for ciliogenesis.

INTRODUCTION

Budding uninhibited by benzimidazole-related 1 (BUBR1) is a central component of the spindle assembly checkpoint and checkpoint signalling. It has been shown that in early M phase, BUBR1 binds to cell division cycle protein 20 (CDC20), a co-activator of the anaphase-promoting complex/cyclosome (APC/C), and inactivates the APC/C^{CDC20} until all chromosomes have made proper attachments to the mitotic spindle (1,2). When all the kinetochores establish bipolar attachment, BUBR1 becomes a substrate of APC/C^{CDC20} and is degraded through ubiquitin-mediated proteolysis (3). It was also reported that BUBR1 binds to CDC20 to inhibit APC/C^{CDC20} activity in G2 phase prior to mitotic onset (4,5). Therefore, BUBR1 functions as a pseudo-substrate inhibitor of APC/C^{CDC20} in G2 to early M phase to prevent unscheduled degradation of specific APC/C^{CDC20} substrates.

APC/C activity is controlled during the cell cycle through the binding of CDC20 or another co-activator, CDC20 homolog 1 (CDH1). CDC20 is expressed during S, G2 and M phases, but only associates with the APC/C during the M phase when several core subunits of the APC/C are phosphorylated by cyclin-dependent kinase1 (CDK1)/cyclin B.

*To whom correspondence should be addressed. Tel: +81 822575809; Fax: +81 822567101; Email: shinya@hiroshima-u.ac.jp

The activated APC/C^{CDC20} initiates the metaphase–anaphase transition through ubiquitin-mediated degradation of securin and cyclin B (6). In the anaphase, CDC20 is released from the APC/C since the core subunits of APC/C are dephosphorylated through the inhibition of CDK1/cyclin B activity, and APC/C^{CDC20} is no longer active by the end of mitosis. In contrast to CDC20, CDH1 is phosphorylated by CDK1/cyclin B during the M phase, and the CDH1 phosphorylation prevents it from binding the core APC/C subunits. Therefore, APC/C^{CDH1} is inactive in early M phase and becomes active from late M to G1 phases once APC/C^{CDC20} has inhibited CDK1/cyclin B activity (6). The activated APC/C^{CDH1} then targets several substrates, including CDC20 and CDH1 itself, to maintain the G1 and G0 phases.

Constitutional mutations in the budding uninhibited by benzimidazoles 1 homolog beta (BUB1B) gene encoding BUBR1 cause a rare human disorder—the premature chromatid separation syndrome [PCS (MIM 176430)], also known as the mosaic variegated aneuploidy (MVA) syndrome (MIM 257300). The PCS (MVA) syndrome is characterized by PCS in >50% metaphase cells, a variety of mosaic aneuploidies (gain or loss of whole chromosomes), severe intrauterine growth and mental retardation, and a high risk of childhood cancers (7,8). Both biallelic (7) and monoallelic (8) mutations of *BUB1B* have been found in individuals with the syndrome that resulted in low overall BUBR1 abundance. The clinical findings in the patients included the Dandy–Walker complex (9/16 patients), postcerebellar cyst (1/16), hypoplasia of the cerebellar vermis (1/16), lissencephaly (1/16), polycystic, often bilateral, nephroblastoma (7/16), polycystic kidney (2/16) and infantile obesity (2/11). These clinical features imply a critical role of BUBR1 in morphogenesis. However, little is known about the function of BUBR1 other than mitotic control. Using cell lines from the patients with the syndrome, we demonstrate that BUBR1 is essential for the formation of primary cilium; a microtubule-based organelle on the surface of most vertebrate cells in G0 phase, and that the PCS (MVA) syndrome is a novel ciliopathy. The primary cilium is regulated by APC/C^{CDH1} activity through ubiquitin-mediated proteolysis of dishevelled (DVL) (9). Therefore, we studied the APC/C activity in G0 phase in the cells from the patients. We demonstrate that BUBR1 has a novel role for the maintenance of the APC/C^{CDH1} activity in G0 phase that regulates the optimal level of DVL for ciliogenesis through proteasomal degradation of CDC20.

RESULTS

PCS (MVA) syndrome, a human condition of BUBR1 insufficiency, is a novel ciliopathy

Patients with the PCS (MVA) syndrome show Dandy–Walker complex, postcerebellar cyst, hypoplasia of the cerebellar vermis, lissencephaly, polycystic, often bilateral, nephroblastoma, polycystic kidney and infantile obesity (Fig. 1A). Since some of the clinical features were suggestive of impaired cilia formation (10–12), we speculated that the PCS (MVA) syndrome has ciliary dysfunction. Therefore, immortalized skin fibroblasts (PCS1 and MY1) from two unrelated patients with the PCS (MVA) syndrome were synchronized with serum starvation at G0 phase, and analysed for ciliogenesis (Fig. 1B and C). As much as 30% of cells from a normal individual (SM) were ciliated, but only 4% of MY1 cells and 1% of PCS1 cells were ciliated. PCS1 cells transferred with a whole chromosome 15 containing the *BUB1B* locus (hereafter called PCS1-Ch.15 cells) (8,13) showed restored ciliogenesis. Primary skin fibroblast cells from the two patients (PCS1sk and MY1sk) (8,13) also showed reduced ciliogenesis, as did Madin–Darby canine kidney (MDCK) cells transfected with a short-interfering RNA (siRNA) targeting *BUB1B* (Supplementary Material, Fig. S1A and C). These results indicate that cells with BUBR1 insufficiency have impaired ciliogenesis, and that the PCS (MVA) is a novel ciliopathy.

Apical docking of basal body is impaired in the PCS (MVA) syndrome

In many cells in G0 phase, centrosomes migrate to the cell surface and are anchored to the membrane (apical docking), and primary cilia are assembled from the basal bodies (12). Immunostaining experiments revealed that in PCS1-Ch.15 cells BUBR1 is localized in the basal body, and that in PCS1 cells the signal for BUBR1 on the centrosome was dramatically reduced (14) (Fig. 1D). We then examined the apical docking of centrosomes under a confocal microscopy to learn how reduced levels of BUBR1 affect ciliogenesis. Centrosomes in cultured revertant PCS1-Ch.15 cells were localized to the apical surface, but those in PCS1 cells failed to dock apically and localized randomly (Fig. 2A–C). Transmission electron microscopy supported that the centrosomes in PCS1 cells failed to localize apically and remained in the cytoplasm (Fig. 2D). These results indicate that BUBR1 is required for apical docking of basal bodies.

BUBR1 in G0 phase is required for APC/C^{CDH1}-mediated proteosomal degradation of DVL

Optimal levels of DVL, a core regulator protein in Wnt signalling, have been shown to be indispensable for apical docking of basal bodies, and both accumulation and attenuation of DVL lead to defective ciliogenesis (9,15,16). We, therefore, examined the levels of DVL1, DVL2 and DVL3 in PCS (MVA) syndrome cells. Since DVL2 is dominantly expressed in PCS1 cells as described below, DVL2 was compared with that of the revertant PCS1-Ch.15 cells. DVL2 was increased in both nuclear and cytoplasmic fractions (Fig. 3A). Primary skin fibroblast cells from these patients (PCS1sk and MY1sk) and *BUB1B* siRNA-transfected MDCK cells all showed increased DVL2 levels (Supplementary Material, Fig. S1B and D). Consistent with the high levels of DVL2, its downstream target, active β-catenin, was increased in a nuclear fraction and increased Wnt signalling was observed in PCS (MVA) syndrome cells (Fig. 3A and Supplementary Material, Fig. S2A–C). Next, we examined whether DVL2 or active β-catenin is involved in ciliary dysfunction in PCS1 cells. Induced expression of DVL2 in PCS1-Ch.15 cells suppressed ciliogenesis (Supplementary Material, Fig. S3C). In addition, knockdown of both DVL2 and DVL3 in PCS1 cells resulted in partial recovery of ciliogenesis (Fig. 4). On the other hand, treatment with Wnt/β-catenin signalling inhibitors, FH535 or

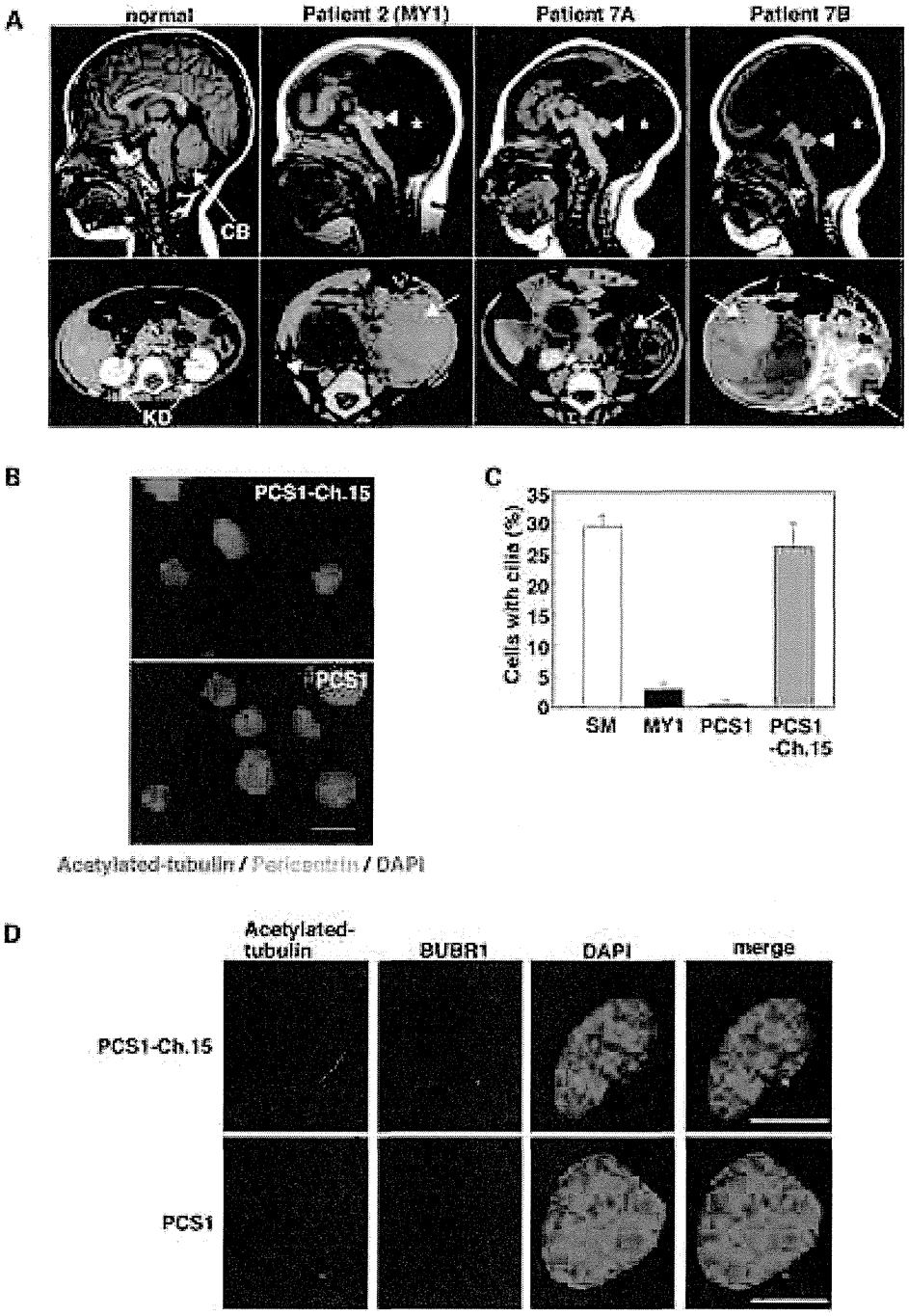

Figure 1. Human PCS (MVA) syndrome is a novel ciliopathy. (**A**) Normal individual. Patients 2, 7A, and 7B (8). MY1 cells used in this study were derived from patient 2 (8). Patients 7A and 7B are the siblings carrying a heterozygous single-base deletion 1833delT, the same mutation as the one found in patient 1 (PCS1), and a conserved haplotype around *BUB1B* that links to a modest decrease in their transcripts (8). Mid-sagittal views of head MRI showing Dandy–Walker complex with hypoplasia of the cerebellar vermis (arrowheads) and enlarged posterior fossae (asterisks). Abdominal CT images of multicystic nephroblastoma (arrows) and a cystic kidney (arrowhead). (**B** and **C**) Analysis of serum starvation-induced ciliogenesis in immortalized fibroblast cells from two patients (PCS1 and MY1) and a normal individual (SM). Both PCS1 and MY1 cells showed decreased ciliated cells. Microcell-mediated transfer of a human chromosome 15 (containing the *BUB1B* locus) restored the reduced ciliogenesis in PCS1 cells (PCS1-Ch.15 cells). Bar: 40 μm. (**D**) Immunofluorescence analyses of BUBR1 and acetylated tubulin in PCS1-Ch.15 cells and PCS1 cells in G0 phase. BUBR1 is localized to the basal body in PCS1-Ch.15 cell, whereas signal for BUBR1 on the basal body was severely reduced in PCS1 cells. Bar: 20 μm.

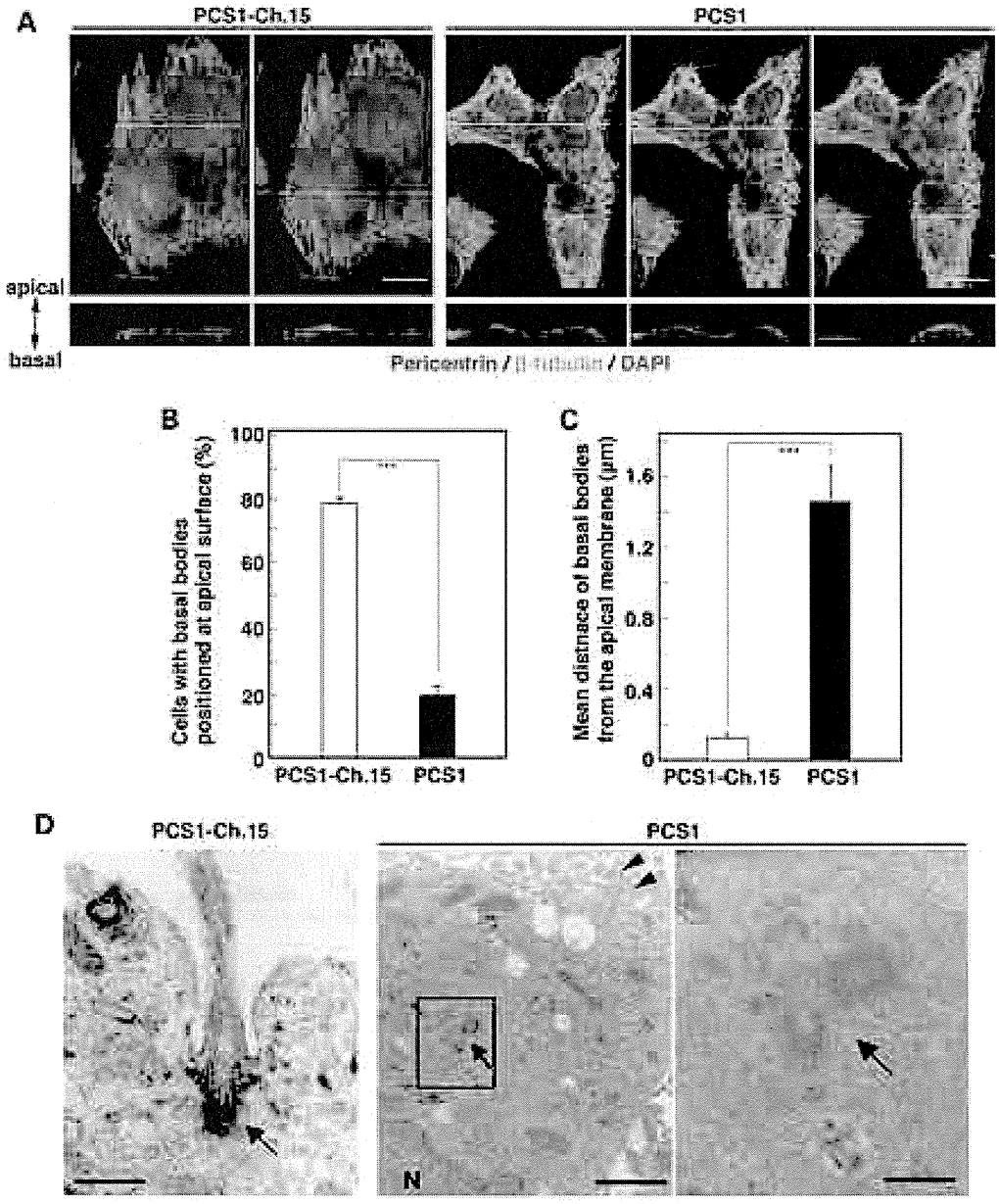

Figure 2. Basal bodies fail to dock at the apical membrane in the PCS (MVA) syndrome. (**A**) Surface view of a three-dimensional confocal microscopic image (upper panel), and cross-section view (lower panel) at an indicated yellow line showing basal bodies (red, Pericentrin), cellular β-tubulin network (green) and nuclei (blue, DAPI). A white-dotted line shows basal position of a cell. PCS1-Ch.15 cells showed localization of the basal bodies to the apical surface of the cells. In contrast, PCS1 cells show randomized localization of the basal bodies. Bar: 40 μm. (**B**) The differences in the apical position of basal bodies were statistically significant (***$P < 0.01$). For each cell line, >100 cells were scored. (**C**) The mean distance of basal bodies from the apical membrane in PCS1 cells was longer than that of PCS1-Ch.15 cells (***$P < 0.01$). For each cell line, 50 cells were examined. (**D**) Transverse sections of PCS1 cells observed with transmission electron microscopy. A PCS1-Ch.15 cell showed normal outgrowth of a ciliary axoneme from a basal body (arrow) docked at the apical membrane (left). In PCS1 cells, centrosomes (arrow) failed to localize apically and remained in the cytoplasm (middle and right). Arrowheads in the middle image show microvilli at the apical membrane. Close inspection of the square region in the middle panel indicated that the PCS1 cell has no typical structure of basal body (right). Bar: 500 nm (left and right image), 1.5 μm (middle image).

inhibitor of Wnt response-1 (IWR-1), in PCS1 cells did not restore ciliogenesis, although Wnt activity was suppressed to the level of PCS1-Ch.15 cells (Supplementary Material, Fig. S2D and E). These results indicate that an excess amount of DVL, but not β-catenin, is associated with the failure of ciliogenesis in PCS (MVA) syndrome cells.

To clarify whether the DVL2 synthesis is enhanced or the DVL2 degradation is decreased in PCS1 cells, the DVL2

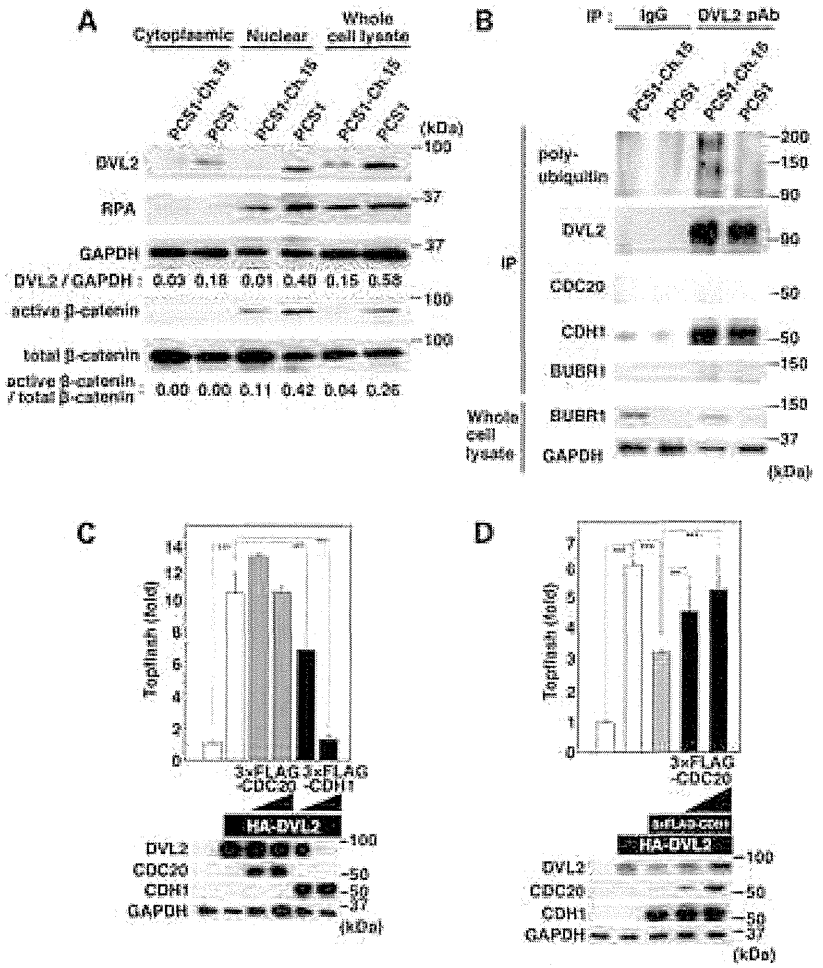

Figure 3. BUBR1 determines the stability of the DVL protein, an APC/C^{CDH1} substrate, through its polyubiquitination. (**A**) Western blot analysis of Wnt signalling components in PCS1 cells. Whole cell lysates were separated to a cytoplasmic and a nuclear fraction. Replication protein A (RPA), a nuclear protein, served as a positive control for the nuclear fractionation. Dishevelled2 (DVL2) was increased in both a nuclear and cytoplasmic fraction from PCS1 cells. Active β-catenin (dephosphorylated form of β-catenin) was also increased in a nuclear fraction of PCS1 cells. The levels of DVL2 and active β-catenin were normalized to those of GAPDH and total β-catenin, respectively. (**B**) Immunoprecipitation and western blot analyses of DVL2 in PCS1 and PCS1-Ch.15 cells. Endogenous DVL2 was immunoprecipitated (IP) using an anti DVL2 polyclonal antibody and analysed for the ubiquitination state by western blotting with anti-FK1 monoclonal antibody. GAPDH served as a loading control. DVL2 was ubiquitinated in PCS1-Ch.15 cells, but the level of DVL2 ubiquitination was reduced in PCS1 cells. DVL2 interacted with CDH1, but not with CDC20 or BUBR1 in both PCS1 and PCS1-Ch.15 cells. These results suggest that APC/C^{CDH1} but not APC/C^{CDC20} mediates the ubiquitination of DVL2 in a BUBR1-dependent manner. (**C**) Serum-starved HEK293T cells were transfected with an hemagglutinin (HA)-DVL2 vector and a 3xFLAG-CDC20 (or CDH1) vector as indicated, and DVL2 levels were analysed by immunoblotting and Wnt signalling activity was analysed using a TCF/LEF-1-dependent luciferase reporter construct (Topflash). Transfection of the HA-DVL2 vector induced a high level of HA-DVL2 expression and Topflash activation. 3xFLAG-CDH1 expression, but not CDC20 expression, significantly suppressed HA-DVL2 expression and Topflash activation. (**D**) CDC20 inhibits APC/C^{CDH1} activity in G0 phase. Serum-starved HEK293T cells were transfected with the HA-DVL2, 3xFLAG-CDH1 and 3xFLAG-CDC20 vector as indicated, and analysed. 3xFLAG-CDC20 expression dramatically induced HA-DVL2 expression and Topflash activation. The statistical significance of the difference was examined by *t*-test. $^{**}P < 0.05$ and $^{***}P < 0.01$.

protein was analysed by western blotting in serum-starved cells after treatment with the protein synthesis inhibitor cycloheximide (Chx) or proteasome inhibitor MG132. The level of DVL2 in PCS1-Ch.15 cells was substantially decreased after Chx treatment and increased after MG132 treatment (Supplementary Material, Fig. S3A). These results indicated that DVL2 is continuously synthesized and degraded in the cells. In contrast, Chx treatment did not decrease the DVL2 level in PCS1 cells, suggesting that the DVL2 synthesis is not increased in PCS1 cells. Additionally, MG132 did not increase the DVL2 level in PCS1 cells, suggesting that proteasome-dependent DVL2 degradation is defective in PCS1 cells. Therefore, we examined the ubiquitination state of DVL2 in PCS1 cells, PCS1-Ch.15 cells and cultured human embryonic

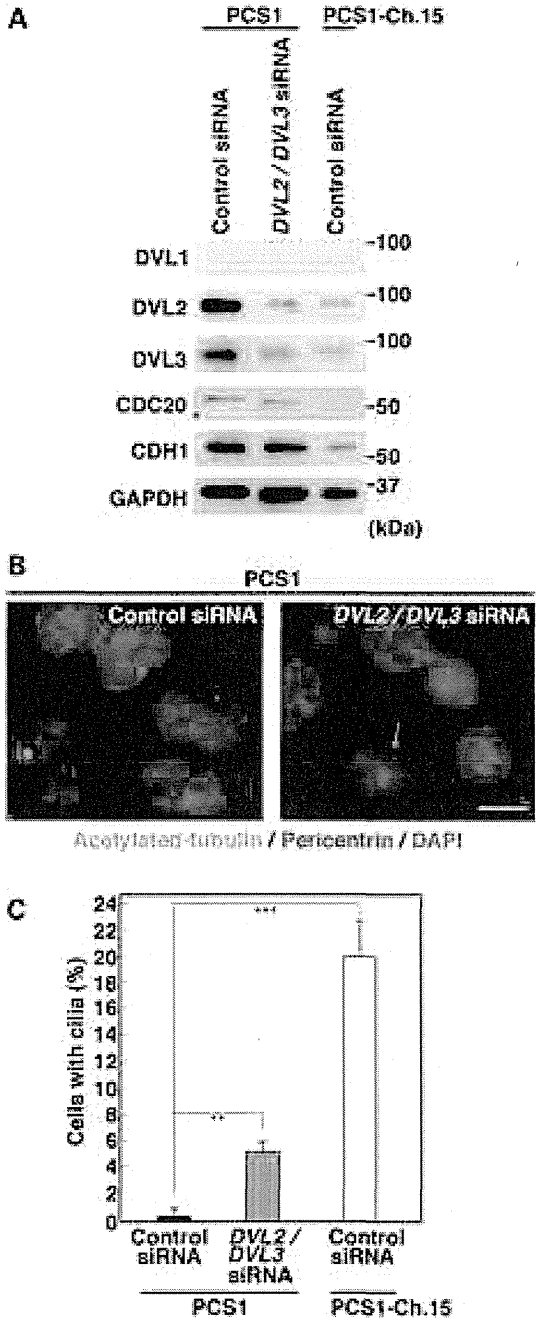

Figure 4. Knockdown of DVL partially restores ciliogenesis in PCS (MVA) syndrome cells. (**A**) Knockdown of *DVL2/DVL3* reduces the expression level of DVLs in PCS1 cells. Western blot analysis of DVLs, CDH1 and CDC20 in PCS1-Ch.15 cells and PCS1 cells after transfection of a siRNA targeting the conserved sequence between *DVL2* and *DVL3*. GAPDH served as a loading control. (**B**) Knockdown of DVL2/DVL3 rescued partially ciliogenesis in PCS1 cells. PCS1 cells transfected with control siRNA or *DVL2/DVL3* siRNA are shown. Primary cilia were stained with an anti-acetylated tubulin antibody (green), centrosomes were stained with an anti-Pericentrin antibody (red) and DNA was stained with DAPI (blue). Bar: 40 μm. (**C**) The differences in ciliogenesis were statistically significant (**$P < 0.05$; ***$P < 0.01$).

kidney (HEK293T) cells. DVL2 was polyubiquitinated in PCS1-Ch.15 cells and normal HEK293T cells, while the ubiquitination level was decreased in PCS1 cells and *BUB1B* knockdowned HEK293T cells (Fig. 3B and Supplementary Material, Fig. S3B). DVLs contain a destruction box (D-box: RXXL) that is recognized by APC/C (9), and an L435S mutation in the D-box inhibited ubiquitination of DVL2 (Supplementary Material, Fig. S3B), suggesting that APC/C ubiquitinates DVL2 in normal cells. Since APC/C activity is controlled through the binding of two co-activators, CDC20 and CDH1 (2), we examined which co-activator is involved in the APC/C-mediated DVL2 proteolysis. Induced expression of CDH1 in HEK293T cells reduced the DVL2 level and suppressed Wnt signalling, while overexpression of CDC20 did not (Fig. 3C), indicating that CDH1, but not CDC20, promotes the APC/C-mediated DVL2 proteolysis. The reduction in the DVL2 level (and Wnt activity) by CDH1 was inhibited by a gradual increase in CDC20 (Fig. 3D), indicating that CDC20 antagonizes the APC/C^{CDH1} activity. These results demonstrated that DVL is degraded through the APC/C^{CDH1}-mediated proteolysis in G0 phase, and BUBR1 is required for the APC/C^{CDH1} activity.

BUBR1 maintains APC/C^{CDH1} activity for ciliogenesis through proteasomal degradation of CDC20

To address the mechanism for the regulation of APC/C^{CDH1} activity by BUBR1, the expressions of CDC20 and CDH1 during the cell cycle were examined. In PCS1-Ch.15 cells, CDC20 was detected in S, G2 and M phases but not in G0 phase, as previously reported in normal cells (1,2). In contrast, in PCS1 cells, CDC20 was highly expressed in G0 phase (Fig. 5A). The proteasome inhibitor MG132 blocked the degradation of CDC20 (and DVL2) in serum-starved PCS1-Ch.15 cells, whereas PCS1 cells showed high levels of CDC20 (and DVL2) even in the absence of MG132 (Supplementary Material, Fig. S4A), suggesting that in G0 phase CDC20 is ubiquitinated in normal cells in a BUBR1-dependent manner. We, therefore, examined the ubiquitination state of CDC20 exogenously expressed in serum-starved normal (HEK293T) cells. CDC20 was polyubiquitinated in serum-starved HEK293T cells, and the ubiquitination level was decreased after BUBR1 depletion (Fig. 5B). CDC20 interacts with CDC27 (APC3), a core subunit of the APC/C, in a BUBR1-dependent manner (Supplementary Material, Fig. S4B). The region comprising residues 490–560 and the D-box motif in BUBR1 is, respectively, required for the binding with CDC20 and CDC27 (APC3) in serum-starved HEK293T cells (Supplementary Material, Fig. S5). These biochemical results suggest that BUBR1–APC/C complex mediates polyubiquitination of CDC20 in quiescent normal cells. As mentioned above, CDC20 antagonized the APC/C^{CDH1} activity in G0 phase. Consistent with this, knockdown of CDC20 in PCS1 cells resulted in a reduction in DVL2 (Fig. 5C) and partial recovery of ciliogenesis (Fig. 5D and E). These results indicate that a high amount of CDC20 in PCS1 cells impairs the APC/C^{CDH1}-mediated DVL2 ubiquitination for ciliogenesis. PCS1 cells also showed high levels of CDH1 in G0 phase (Fig. 5A). Although BUBR1 in G0 phase did not bind to CDH1 directly, the interaction of CDH1 with

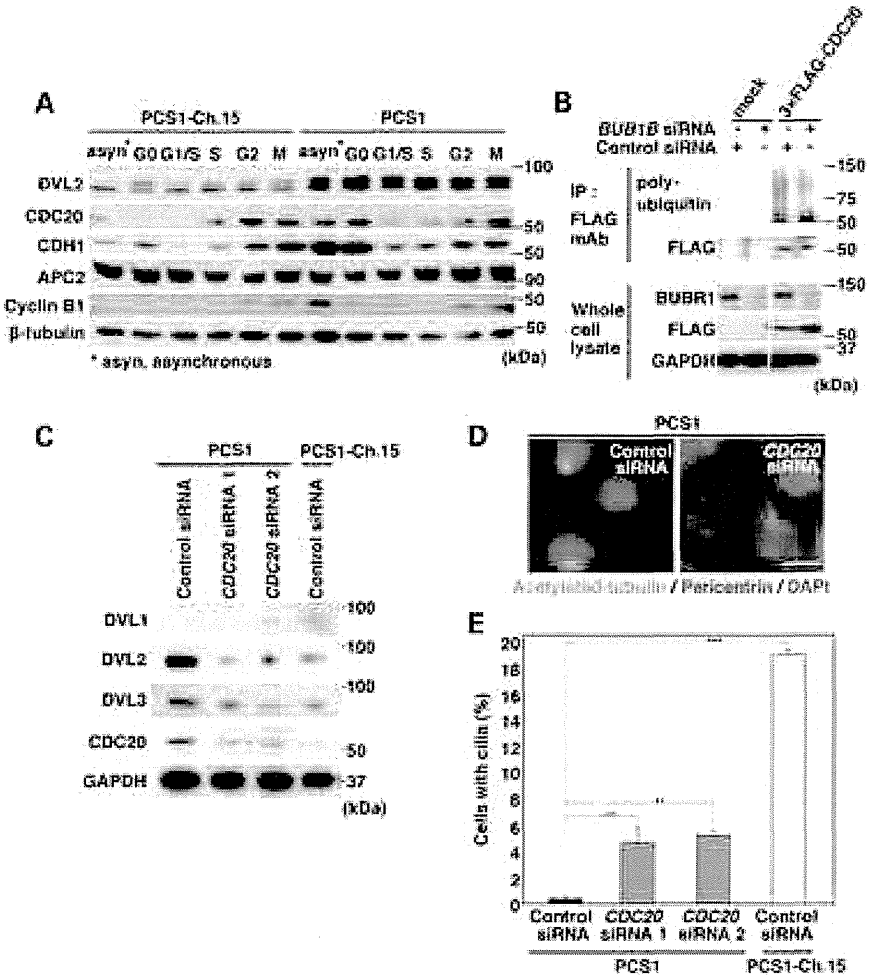

Figure 5. BUBR1-dependent CDC20 proteasomal degradation in G0 phase is required for ciliogenesis. (**A**) Levels of APC/C components during the cell cycle were analysed by western blotting. High levels of CDC20 and CDH1 were observed in PCS1 cells in the G0 phase. (**B**) BUBR1 is required for CDC20 ubiquitination in G0 phase. 3xFLAG-CDC20 and *BUB1B* siRNA (or control siRNA) were co-transfected into HEK293T cells. After serum starvation for 24 h, whole cell lysates were immunoprecipitated (IP) with anti-FLAG antibody, and the polyubiquitination state of CDC20 was evaluated by immunoblotting with anti-FK1 monoclonal antibody. *BUB1B* knockdown reduces the level of CDC20 ubiquitination. APC/C^{CDH1}, not APC/C^{CDC20}, is responsible for ubiquitin-mediated degradation of DVL2 in G0 phase. (**C**) Knockdown of *CDC20* reduces the expression level of DVL2 in PCS1 cells. Western blot analysis of DVLs in PCS1 cells after transfection of *CDC20* siRNA and PCS1-Ch.15 cells. GAPDH served as a loading control. The expression levels of DVL2 were decreased after transfection of *CDC20* siRNA. (**D**) Knockdown of CDC20 partially restored ciliogenesis in PCS1 cells. PCS1 cells transfected with control siRNA or *CDC20* siRNA are shown. Primary cilia were stained with an anti-acetylated tubulin antibody (green), centrosomes were stained with an anti-Pericentrin antibody (red) and DNA was stained with DAPI (blue). Bar: 40 μm. (**E**) The differences in ciliogenesis were statistically significant (**$P < 0.05$; ***$P < 0.01$).

APC/C was impaired significantly after BUBR1 depletion in HEK293T cells (Supplementary Material, Fig. S4B). Since CDH1 is autonomously degraded by APC/C^{CDH1} during G0 phase (17), the high levels of CDH1 might be the consequence of the decreased APC/C^{CDH1} activity in PCS1 cells. Based on these results, we propose a model that in G0 phase BUBR1 binds to CDC20 (Supplementary Material, Fig. S4B) (18) to inhibit APC/C^{CDC20} and instead activates APC/C^{CDH1}, thereby allowing DVL proteasomal degradation to establish its optimal level for ciliogenesis (Fig. 6).

Medaka *bubr1* insufficiency causes ciliary dysfunction characterized by defects in cerebellum formation and perturbed left–right axis

To learn whether the functional role of BUBR1 for ciliogenesis is conserved in vertebrates, we induced BUBR1 insufficiency in medaka fish (*Oryzias latipes*) (19). *bubr1* (medaka homolog of *BUB1B*) expression is ubiquitous under normal conditions (Fig. 7A). Knockdown of *bubr1* with two distinct antisense morpholino oligonucleotides (knockdown efficacy

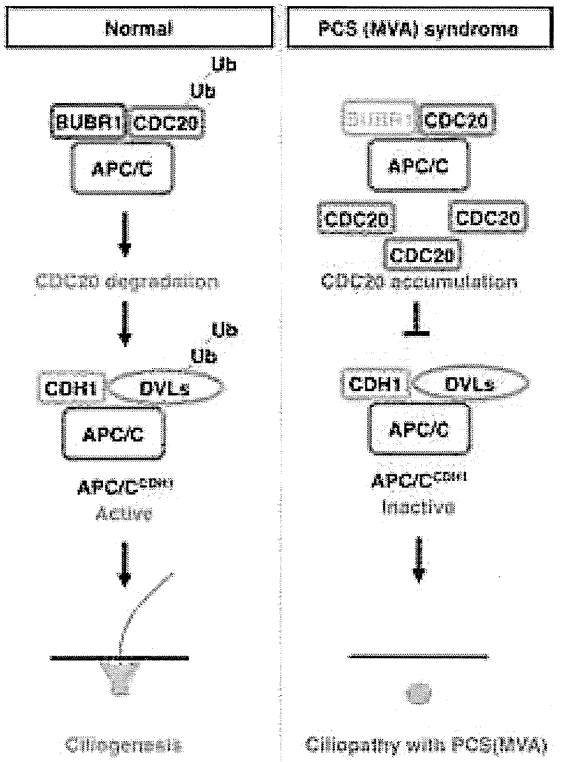

Figure 6. A model of the molecular function of BUBR1 in ciliogenesis. BUBR1-dependent CDC20 degradation in G0 phase cells plays a role in the maintenance of APC/C^{CDH1} activity during primary cilia formation. In PCS (MVA) syndrome cells, insufficiency of BUBR1 results in CDC20 accumulation to inhibit APC/C^{CDH1} activity in G0 phase. Excess amounts of DVLs, the targets of APC/C^{CDH1}, interfere apical docking of centrosomes to cause impaired ciliogenesis.

and specificity are shown in Fig. 7D and Supplementary Material, Figs. 6 and 7) perturbed the formation of the cerebellum (Fig. 7B), as observed in patients with the PCS (MVA) syndrome. *bubr1* morphants also showed perturbed left–right asymmetry of visceral organs including the liver, spleen, gut and cardiac looping (Fig. 7C and D and Supplementary Material, Fig. S7), although no patients with the syndrome with perturbed left–right asymmetry have been reported. Randomized expression of left–right asymmetry genes was observed, including the nodal ligand *southpaw* (*spaw*) and its downstream genes *lefty* and *pitx2* in the lateral plate mesoderm, which comprise the readout of cilium-generated fluid flow in Kupffer's vesicle, a teleost-specific organ equivalent to a mouse node (Supplementary Material, Fig. S8). The number of cilia in Kupffer's vesicle was significantly reduced (Fig. 7E and F), resulting in defective fluid flow (Fig. 7E and G and Supplementary Material, Movies S1 and S2). These results demonstrate a conserved role of BUBR1 for the primary cilium formation, but also suggest phenotypic heterogeneity between human and medaka fish.

DISCUSSION

In mammalian cells, failure of spindle microtubule–kinetochore attachments in M phase activates BUBR1 to bind to CDC20 and inhibit APC/C^{CDC20}, leading to inhibition of chromosome separation (1,2,18,20). Although the inhibition of CDC20 by BUBR1 for spindle assembly checkpoint in M phase has been well established (1–5), the role of BUBR1 in G0 phase was unclear. We found that BUBR1 binds to CDC20 and the core APC/C subunits and forms a complex in G0 phase, and that siRNA-knockdown of BUBR1 in HEK293T cells impairs poly-ubiquitination of CDC20. These results demonstrate that in G0 phase BUBR1 inhibits APC/C^{CDC20} activity through the proteasomal degradation of CDC20. Accumulation of CDC20 was observed in the PCS (MVA) syndrome cells, but was not likely to be the mitotic leakage, because in late M phase active APC/C^{CDC20} causes its own inhibition and switches to APC/C^{CDH1} activity independently of spindle assembly checkpoint (21). It was recently reported that BUBR1 binds to CDC20 to inhibit APC/C^{CDC20} in interphase, thereby allowing accumulation of cyclin B in G2 phase prior to mitotic onset (4,5). Thus, BUBR1 may function as an inhibitor of APC/C^{CDC20} not only in early M phase but also in multiple phases of the cell cycle.

Conditional knockdown of *APC2*, a core subunit of APC/C, in G0-quiescent hepatocytes in mice caused dedifferentiation and unscheduled proliferation of these cells, which may be attributed to the lack of APC/C^{CDH1} activity (22). APC/C^{CDH1} activity regulates axonal growth in postmitotic neurons (23). In the context of cilia formation, APC/C^{CDH1} activity is indispensable for apical docking of basal body through the quantitative regulation of DVL by APC/C^{CDH1} in *Xenopus* embryos (9). CDC14 phosphatases in vertebrates, *CDC14A* and *CDC14B*, both counteract CDH1 phosphorylation to activate APC/C^{CDH1} activity during late M phase (24). Loss of *CDC14B* in zebrafish embryos caused ciliary dysfunction characterized by hydrocephaly, kidney cysts and left–right asymmetry defects (25). These findings suggested that APC/C^{CDH1} activity in G0 phase is essential for cell differentiation and cell morphology (26). In spite of the functional significance of APC/C^{CDH1}, the maintenance mechanism in G0 phase was unclear. We showed that the accumulation of CDC20 in G0 phase interferes with the APC/C^{CDH1}-mediated proteolysis of DVL for ciliogenesis, and that BUBR1 is required for the maintenance of the APC/C^{CDH1} activity in G0 phase.

The 'APC/C^{CDH1}–DVL proteolysis' axis in G0 phase is fundamental for ciliogenesis. Our data demonstrated that BUBR1 in G0 phase maintains the APC/C^{CDH1} activity to establish the 'BUBR1–APC/C^{CDH1}–DVL proteolysis' axis for ciliogenesis. It was reported that inversin (NPHP2), an underlying protein for the ciliopathy in both human and mouse, binds to DVL and promotes the ubiquitination of DVL by APC/C^{CDH1} (15). Loss of *inversin* leads to increased amounts of DVL and ciliary dysfunction similarly to the PCS (MVA) syndrome. Therefore, the PCS (MVA) syndrome and inversin-mutated ciliopathy (nephronophthisis) may have a common pathological pathway, and BUBR1 may act epistatically upstream of both inversin and DVL to maintain APC/C^{CDH1} activity for ciliogenesis, because inversin is also a direct substrate of APC/C^{CDH1} (15).